A Two-Wheeled Robot Trajectory Tracking Control System Design Based on Poles Domination Approach

Nur Uddin, *Member, IAENG*

***Abstract*—A trajectory tracking control system design of mobile robot based on poles domination approach is presented. A two-wheeled robot is used as a study case in deriving the method. Trajectory tracking problem of the robot is formulated as a stabilization problem of the robot posture error dynamics. A state feedback control system is applied in stabilizing the posture error dynamics. The state feedback control law is designed by approximating the posture error dynamics as a third order linear system. A control gain matrix is obtained through factorizing the closed loop system characteristic into a first and a second order systems. Elements of the control matrix are determined by defining the desired closed loop system characteristic, i.e: time constant, system damping, and natural frequency. Domination of the first order system part and the second order system part in the closed loop system are evaluated through computer simulations. The results show that domination of the second order system part resulted in better tracking performance than domination of the first order system part. This presented method offers a simple technique for designing a mobile-robot trajectory tracking system.**

***Index Terms*—Autonomous mobile robot, two-wheeled robot, trajectory tracking control, control design, poles domination.**

I. Introduction

Autonomous mobile robot (AMR) is one of the most interesting research topics in the last three decades. The AMR is a mobile robot that is able to move autonomously from one location to another location. The AMR is equipped with a trajectory tracking control system (TTCS) that acts as a driver to steer the robot. The TTCS integrates a navigation system and a control system. The navigation system is to determine current positions and orientation of the robot. The position and orientation of the robot are known as the robot posture. The current posture robot is compared to the desired posture, and the different is known as the posture error. The control system is applied to minimize the posture error such that the robot posture approaches to the desired posture.

Mobile robots have several types and include ground mobile robot, aerial mobile robot, water-surface mobile robot, and underwater mobile robot. A study on developing autonomous ground mobile robot was firstly reported by Kanayama et al. in [1]. They developed an autonomous four-wheeled robot. The robot has two active wheels and two passive wheels. A TTCS was developed to make the robot move autonomously. The TTCS was designed using the Lyapunov-base control method based. The experimental results show that the robot was able to move on a desired route to reach a destination. Since then, several studies on developing autonomous four-wheeled robot were presented by applying different control methods, for examples: back-stepping control [2], [3], Lyapunov direct's method [4], [5], sliding mode control [6], adaptive control [7], and particle swarm optimization [8].

Another interesting ground mobile robot is a two-wheeled robots (TWR). The TWR is a ground mobile robot where the robot body is supported by two active wheels only. The wheels are driven by two independent high-torque electric motor. Utilizing two wheels only makes maneuverability of the TWR higher than the four wheeled robot. However, the TWR is statically unstable due to the two wheels usage. Thanks to the active stabilizing system for solving the TWR instability problem. The active stabilization system is a state feedback control system for actively stabilizing the TWR. The TWR is very potential in developing autonomous vehicle with high maneuverability.

An autonomous TWR was firstly presented in [9]. The TWR was able to move autonomously on a desired straight line path from indoor to outdoor as reported in the experimental results. The control system was designed using the optimal control method. The control system consisted of two control loops: active stabilization (balancing) control loop and trajectory tracking control loop. Both control loops accommodated three control tasks: balancing and speed control, steering control, and straight line tracking control. The experimental test results showed that coupling between the both control loops is low and neglect-able for small angular velocity of heading motion. The other studies on autonomous two wheel robot have also been presented by applying different control methods. A development of autonomous TWR by applying partial states feedback linearization control was presented in [10]. Adapative control scheme was studied to overcome parameter uncertainties in autonomous TWR, for examples: adaptive backstepping control [11], adaptive sliding mode control [12], and neural networks [13].

An observation showed that the presented autonomous TWRs were designed to track a certain set of desired position or velocities, but not an arbitrary trajectory in an earth-fixed coordinate system [14]. A certain set data of desired position or velocities have to be defined before operating the autonomous TWR. It is quite practical in real application. Defining the desired trajectory in earth-fixed coordinate system is more practically as it is can be integrated with modern navigation system, for example: global positioning system (GPS). Yue et al. presented an autonomous TWR that is able to track an arbritrary trajectory in earth-fixed coordinate system [14]. Model predictive control (MPC) was applied in designing TTCS of the autonomous TWR. Another

Manuscript received May 02, 2019; revised Dec 22, 2019.

N. Uddin is with the Department of Informatics, Universitas Pembangunan Jaya, Tangerang Selatan, 15413 Indonesia, e-mail: nur.uddin@upj.ac.id.

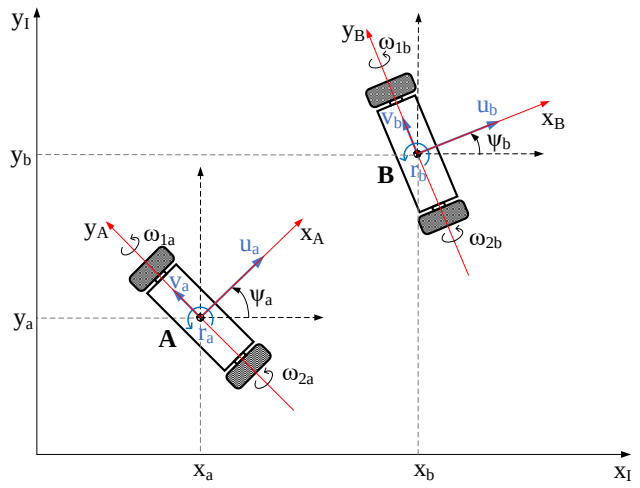

Fig. 1. TWR coordinate systems.

study on TWR tracking control system in a earth-fixed frame coordinate system by has also been reported in [15], where the TTCS was designed using optimal control method.

This paper presents a design of TTCS for autonomous TWR based on the system poles domination. Goal of the study is to obtain a simple controller that is implementable in a low cost microcontroller. The TWR is assumed to be stabilized where the TWR stabilization system can adopt, for examples [16]–[19]. Moreover, coupling between control loops of the stabilization system and the TTCS is neglected. Presentation of the paper is organized as follows. Section I describes introduction, literature review, and motivation of the work. Section II presents the derivation of trajectory tracking control problem as a stabilization problem of posture error dynamics. Section III described the TTCS design based on the system pole domination. Section IV provides simulation results of applying the designed TTCS and the performance analysis. Section V discusses comparison of the locally asymptotically stable trajectory tracking system and the globally asymptotically stable trajectory tracking system. Finally, conclusion is presented in Section VI. This paper is an extended work of [20] by providing more detail explanation of the method, more simulation results, and performance comparison of the locally asymptotic stable (LAS) and the globally asymptotically stable (GAS) trajectory tracking control systems.

II. Trajectory Tracking Problem

Two units of two-wheeled robot (TWR) on a planar space are shown in Figure 1. Both robots are named the TWR A and the TWR B. Trajectory of the TWR B is defined as the reference trajectory for the TWR A such that the TWR A is desired to track the TWR B movement.

Three coordinate systems are defined to describe position and orientation of both robots as shown in Figure 1. The three coordinate systems are the inertial coordinate system ($x_I y_I$), the TWR A body coordinate system ($x_A y_A$), and the TWR B body coordinate system ($x_B y_B$). The inertial coordinate system is a fixed frame coordinate system where the origin is located at a defined point. Both TWR A and TWR B body coordinate systems is sticking on the robot body and move along with the robot movements. Origin of the robot body coordinate system is usually located at the center mass of the robot. The three coordinate systems are used to express position and orientation of the robots. The robot position describes location of the robot with respect to a reference, while the robot orientation describes the robot heading angle with respect to the reference. The inertial coordinate system as a fixed frame coordinate system is commonly used as the reference for determining the position and orientation. Position and orientation of the robot is also known as the robot posture.

Let both TWRs are moving on the planar space. The TWR A moves with linear velocity u_a and angular velocity r_a, while the TWR B moves linear velocity u_b and angular velocity r_b. The TWR velocities are expressed in the TWR body coordinate system, where the linear velocity is inline to the x-axis and the angular velocity axis is inline to the z-axis as shown in the Figure 1. The TWR A velocities can be expressed into the inertial coordinate system by the following relation:

$$\begin{aligned} \dot{x}_a &= u_a \cos\psi_a \\ \dot{y}_a &= u_a \sin\psi_a \\ \dot{\psi}_a &= r_a. \end{aligned} \tag{1}$$

Expressing the TWR B velocities in the inertial coordinate system is given as follows:

$$\begin{aligned} \dot{x}_b &= u_b \cos\psi_b \\ \dot{y}_b &= u_b \sin\psi_b \\ \dot{\psi}_b &= r_b. \end{aligned} \tag{2}$$

Based on the Figure 1, postures of the TWR A and TWR B at an instant time is defined with respect to the inertial coordinate system as follows:

$$\xi_a = \begin{bmatrix} x_a \\ y_a \\ \psi_a \end{bmatrix} \quad \text{and} \quad \xi_b = \begin{bmatrix} x_b \\ y_b \\ \psi_b \end{bmatrix}, \tag{3}$$

where ξ_a is the posture of TWR A, x_a and y_a is the position of TWR A, ψ_a is the heading angle of TWR A, ξ_b is the posture of TWR B, x_b and y_b is the position of TWR B, and ψ_b is the heading angle of TWR B.

The TWR A is tracking the TWR B trajectory if the TWR A posture approaches the TWR B posture. Deviation of the TWR A posture with respect to the TWR B posture is called the posture error and defined as follows:

$$\xi_e = \xi_b - \xi_a = \begin{bmatrix} x_e \\ y_e \\ \psi_e \end{bmatrix} = \begin{bmatrix} x_b - x_a \\ y_b - y_a \\ \psi_b - \psi_a \end{bmatrix}, \tag{4}$$

where ξ_e is the posture error of TWR A with respect to the TWR B, x_e and y_e are the position deviation of TWR A from the TWR B position, and ψ_e is the heading angle deviation of TWR A with respect to the TWR B heading angle. The posture error is desired to be minimum such the TWR A posture approaches the TWR B posture. Zero posture error is an ideal condition where the TWR A posture is exactly the same as the the TWR B posture. When the posture error is not equal to zero, the TWR A needs to correct its posture to vanish the error. Since the posture error in (4) is expressed in the inertial coordinate system ($x_I y_I$), it is more convenience to transform the posture error into the the TWR A body coordinate system ($x_A y_A$). Transformation of the posture

error from the inertial coordinate system into the TWR A body coordinate system is done using the following relation:

$$\xi_{e_A} = R_{AI}\xi_e, \tag{5}$$

where ξ_{e_A} is the posture error represented in the TWR A body coordinate system, R_{AI} is the transformation matrix from the inertial coordinate system into the TWR A body coordinate system, and ξ_e is the posture error represented in the inertial coordinate system as given in (4). There variables are defined as follows:

$$\xi_{e_A} = \begin{bmatrix} x_{e_A} \\ y_{e_A} \\ \psi_{e_A} \end{bmatrix} \tag{6}$$

and

$$R_{AI} = \begin{bmatrix} \cos\psi_a & \sin\psi_a & 0 \\ -\sin\psi_a & \cos\psi_a & 0 \\ 0 & 0 & 1 \end{bmatrix}. \tag{7}$$

Substituting (4), (6) and (7) into (5) results in:

$$\begin{bmatrix} x_{e_A} \\ y_{e_A} \\ \psi_{e_A} \end{bmatrix} = \begin{bmatrix} \cos\psi_a & \sin\psi_a & 0 \\ -\sin\psi_a & \cos\psi_a & 0 \\ 0 & 0 & 1 \end{bmatrix} \begin{bmatrix} x_b - x_a \\ y_b - y_a \\ \psi_b - \psi_a \end{bmatrix} \tag{8}$$

Since the TWR A and TWR B are moving, the TWR postures and the posture error are time varying. Dynamics of the posture error is given by time derivative of the posture error ξ_{e_A} as follows:

$$\dot{\xi}_{e_A} = \dot{R}_{AI}\xi_e + R_{AI}\dot{\xi}_e \tag{9}$$

and through a further calculation results in [15]:

$$\begin{bmatrix} \dot{x}_{e_A} \\ \dot{y}_{e_A} \\ \dot{\psi}_{e_A} \end{bmatrix} = \begin{bmatrix} r_a y_{e_A} + u_b \cos\psi_{e_A} - u_a \\ -r_a x_{e_A} + u_b \sin\psi_{e_A} \\ r_b - r_a \end{bmatrix}. \tag{10}$$

The (10) is the posture error dynamics of TWR A with respect to the TWR B expressed in the TWR A coordinate system. The posture error is decreasing and vanish if the posture error dynamics is asymptotically stable. The (10) has two manipulated variables, u_a and r_a, to make it asymptotic stable. The trajectory tracking problem is hereby formulated as a stabilization problem of the posture error dynamics.

III. Trajectory Tracking Control System Design

A state feedback control is applied to stabilize the posture error dynamics. The posture error dynamics represented in (10) are a non-linear dynamic system. Assuming the heading angle error (ψ_{e_A}) is small, the non-linear system (10) can be approximated by the following linear system:

$$\begin{bmatrix} \dot{x}_{e_A} \\ \dot{y}_{e_A} \\ \dot{\psi}_{e_A} \end{bmatrix} = \begin{bmatrix} r_a y_{e_A} + u_b - u_a \\ -r_a x_{e_A} + u_b \psi_{e_A} \\ r_b - r_a \end{bmatrix}. \tag{11}$$

Define a state vector

$$\xi_{e_A} = \begin{bmatrix} x_{e_A} \\ y_{e_A} \\ \psi_{e_A} \end{bmatrix} \tag{12}$$

and therefore the (11) can be expressed into the following equation:

$$\dot{\xi}_{e_A} = G\xi_{e_A} + H\mu, \tag{13}$$

where $\dot{\xi}_e$ is the time derivative of system states vector, G is the system matrix, H is the input matrix, and μ is the system input vector, and they are defined as follows:

$$G = \begin{bmatrix} 0 & r_a & 0 \\ -r_a & 0 & u_b \\ 0 & 0 & 0 \end{bmatrix}, H = \begin{bmatrix} 1 & 0 \\ 0 & 0 \\ 0 & 1 \end{bmatrix},$$

$$\mu = \begin{bmatrix} \mu_1 \\ \mu_2 \end{bmatrix} = \begin{bmatrix} u_b - u_a \\ r_b - r_a \end{bmatrix}.$$

Assume that the TWR A is initially at idle position on the planar space, where $u_a = 0$ and $r_a = 0$. Using this assumption, the system matrix of (13) to be:

$$G = \begin{bmatrix} 0 & 0 & 0 \\ 0 & 0 & u_b \\ 0 & 0 & 0 \end{bmatrix}, \tag{14}$$

where the system matrix eigenvalues are $\lambda_1 = 0$, $\lambda_2 = 0$, and $\lambda_3 = 0$. The three eigenvalues are the open loop system eigenvalues of (13).

Now, define the system input vector of (13) as follows:

$$\mu = -K\xi_{e_A} \tag{15}$$

where K is a control gain matrix and the matrix elements are defined as follows:

$$K = \begin{bmatrix} k_{11} & k_{12} & k_{13} \\ k_{21} & k_{22} & k_{23} \end{bmatrix}. \tag{16}$$

Substituting (15) into (13) results in:

$$\dot{\xi}_{e_A} = (G - HK)\xi_{e_A}. \tag{17}$$

The (17) is the closed loop trajectory tracking control system. The closed loop trajectory tracking control system matrix is defined as follows:

$$G_{cl} = G - HK \tag{18}$$

and substituting (14), (16) and the matrix H of of (13) into (18) results in:

$$G_{cl} = G - HK = \begin{bmatrix} -k_{11} & -k_{12} & -k_{13} \\ 0 & 0 & u_b \\ -k_{21} & -k_{22} & -k_{23} \end{bmatrix}. \tag{19}$$

Characteristic of the closed loop system (17) is determined by eigenvalues of G_{cl}. The eigenvalues are obtained by solving the following equation:

$$\det(\lambda I - G_{cl}) = \begin{vmatrix} \lambda + k_{11} & k_{12} & k_{13} \\ 0 & \lambda & -u_b \\ k_{21} & k_{22} & \lambda + k_{23} \end{vmatrix} = 0, \tag{20}$$

where $\det()$ is the mathematics operator for calculating determinant of a matrix, λ are the eigenvalues, and I is an identity matrix. The closed loop system (17) is asymptotically stable if all of the eigenvalues have negative real part. The control gain matrix K is manipulable to make the closed loop system matrix asymptotically stable. The closed loop system matrix can be simplified by defining $k_{12} = 0$, $k_{13} = 0$, and $k_{21} = 0$ such that the control gain matrix K in (16) to be:

$$K = \begin{bmatrix} k_{11} & 0 & 0 \\ 0 & k_{22} & k_{23} \end{bmatrix}. \tag{21}$$

and the closed loop system matrix (20) becomes:

$$G_{cl} = \begin{bmatrix} -k_{11} & 0 & 0 \\ 0 & 0 & u_b \\ 0 & -k_{22} & -k_{23} \end{bmatrix}. \quad (22)$$

Eigenvalues of (22) are obtained by solving the following equation:

$$\det\left(\lambda I - G_{cl}\right) = \begin{vmatrix} \lambda + k_{11} & 0 & 0 \\ 0 & \lambda & -u_b \\ 0 & k_{22} & \lambda + k_{23} \end{vmatrix} = 0 \quad (23)$$

that can be represented as follows:

$$(\lambda + k_{11})\left(\lambda^2 + k_{23}\lambda + u_b k_{22}\right) = 0. \quad (24)$$

The (24) is the characteristics equation of the closed loop system (17).

The characteristic equation (24) is a third order system and factorized into a first order system and a second order system. A third order dynamics system is generally expressed in the following form:

$$\left(\lambda + \frac{1}{\tau}\right)\left(\lambda^2 + 2\zeta\omega_n\lambda + \omega_n^2\right) = 0, \quad (25)$$

where τ is the time constant, ζ is the system damping coefficient, and ω_n is the system natural frequency. The third order system is composed of a first order system and a second order system. Therefore, the third order system response is a combination of the first order system response and the second order system response. Stability of the third order system is determined by stability of the first order system and the second order system. Asymptotically stable of the third order system can be achieved if and only if both the first order system and the second order system are asymptotically stable.

The first order system part of (25) is expressed by:

$$\lambda + \frac{1}{\tau} = 0. \quad (26)$$

Denote eigenvalue of the first order system as λ_1 and therefore $\lambda_1 = -\frac{1}{\tau}$. The first order system is asymptotically stable for the negative eigenvalue. It can be achieved by selecting a positive time constant, $\tau > 0$.

The second order system part of (25) is described by:

$$\lambda^2 + 2\zeta\omega_n\lambda + \omega_n^2 = 0. \quad (27)$$

Let λ_2 and λ_3 are eigenvalues of the second order system. Both eigenvalues are generally expressed as follows:

$$\lambda_{2,3} = -\zeta\omega_n \pm j\omega_n\sqrt{1-\zeta^2}, \quad (28)$$

where j is an imaginary number, $j = \sqrt{-1}$. The second order system is asymptotically stable if the eigenvalues have negative real part, i.e., $\mathrm{Re}(\lambda_2) < 0$ and $\mathrm{Re}(\lambda_3) < 0$, where the $\mathrm{Re}()$ is a mathematics operator to get the real part of a complex number. Both λ_2 and λ_3 have the same real part given as follows:

$$\mathrm{Re}(\lambda_2) = \mathrm{Re}(\lambda_3) = -\zeta\omega_n \quad (29)$$

The (29) implicates that the stability of the second order system is determined by the system damping ζ and natural frequency of the system ω_n. Since the natural frequency is always positive, stability of the second order system is solely determined by the system damping. The second order system is asymptotically stable if the system damping is positive, $\zeta > 0$, such that eigenvalues of the system have negative real number.

Comparing the (24) and the (25) shows that $k_{11} = \frac{1}{\tau}$, $k_{23} = 2\zeta\omega_n$, and $u_b k_{22} = \omega_n^2$. Since ω_n^2 is a non negative number, the u_b and k_{22} have to be in the same sign. Asymptotic stability of the (24) is achieved by control gain matrix (21) with the following criteria:

$$\begin{aligned} &k_{11} > 0 \\ &k_{23} > 0 \\ &u_b k_{22} > 0. \end{aligned} \quad (30)$$

For certain condition, the third order system response may be dominated by either the first order system response or the second order system response. Domination of the first order system is indicated by an eigenvalue that is located closer to imaginary axis than the two other eigenvalues. While, the domination of the second order system is indicated by a pair of complex conjugate eigenvalues that is located closer to the imaginary axis than another eigenvalue. Eigenvalues located close to the imaginary axis are known as the dominant poles.

IV. Simulation and Results

A trajectory tracking control system (TTCS) is designed by applying the control gain matrix (21). Performance of the TTCS is demonstrated through computer simulation with the following scenario. Two units of two-wheeled robot (TWR) named the TWR A and the TWR B are on a planar space. The TWR A is initially located at $(-0.5, 1)$ in an inertial coordinate system with heading angle $90°$. While, the TWR B is initially located at $(0, 0)$ in the inertial coordinate system with heading angle $0°$. The heading angle is measured with respect to x-axis of the inertial coordinate system. Therefore, initial postures of the TWR B and TWR A are denoted by $\xi_b(0) = [0, 0, 0°]^T$ and $\xi_a(0) = [-0.5, 1, 90°]^T$, respectively. Deviation of the TWR A initial posture with respect to the TWR B initial posture is known as the initial posture error and expressed as follows:

$$\xi_e(0) = \xi_b(0) - \xi_a(0) = \begin{bmatrix} 0.5 \\ -1 \\ -90° \end{bmatrix}. \quad (31)$$

The TWR B is simulated moving for 2π seconds at a constant linear velocity, $u_b = 1$ m/s but varying angular velocity ω_b given as follows:

$$\omega_b(t) = \begin{cases} 1 \text{ rad/s} & \text{for } 0 < t \leq \pi \\ -1 \text{ rad/s} & \text{for } \pi < t \leq 2\pi \end{cases} \quad (32)$$

where t is the simulation time. The TWR B is defined to be a reference for the TWR A movement. The TWR A is equipped with the TTCS and desired to track the TWR B movement trajectory.

Control law of the TTCS was defined in (15) and rewritten as follows:

$$\mu = -K\xi_{e_A}, \quad (33)$$

where ξ_{e_A} is the posture error represented in the TWR A body coordinate system (5) and K is the control gain matrix (21). Elements of the control gain matrix are determined based on the criteria in (30). Six controllers of TTCS

TABLE I
THE DESIGNED TRAJECTORY TRACKING CONTROL SYSTEM BASED ON POLE DOMINATION APPROACH

Controller	Desired characteristic	Control gain matrix (K)	Closed loop poles
1a	$\tau = 1$ $\zeta = 0.2$ $\omega_n = 10$	$\begin{bmatrix} 1 & 0 & 0 \\ 0 & 100 & 4 \end{bmatrix}$	$\lambda_1 = -1$ $\lambda_{2,3} = -2 \pm j9.798$
1b	$\tau = 0.2$ $\zeta = 0.2$ $\omega_n = 10$	$\begin{bmatrix} 5 & 0 & 0 \\ 0 & 100 & 4 \end{bmatrix}$	$\lambda_1 = -5$ $\lambda_{2,3} = -2 \pm j9.798$
1c	$\tau = 0.1$ $\zeta = 0.2$ $\omega_n = 10$	$\begin{bmatrix} 10 & 0 & 0 \\ 0 & 100 & 4 \end{bmatrix}$	$\lambda_1 = -10$ $\lambda_{2,3} = -2 \pm j9.798$
2a	$\tau = 1$ $\zeta = 0.7$ $\omega_n = 10$	$\begin{bmatrix} 1 & 0 & 0 \\ 0 & 100 & 14 \end{bmatrix}$	$\lambda_1 = -1$ $\lambda_{2,3} = -7 \pm j7$
2b	$\tau = 0.2$ $\zeta = 0.7$ $\omega_n = 10$	$\begin{bmatrix} 5 & 0 & 0 \\ 0 & 100 & 14 \end{bmatrix}$	$\lambda_1 = -5$ $\lambda_{2,3} = -7 \pm j7$
2c	$\tau = 0.1$ $\zeta = 0.7$ $\omega_n = 10$	$\begin{bmatrix} 10 & 0 & 0 \\ 0 & 100 & 14 \end{bmatrix}$	$\lambda_1 = -10$ $\lambda_{2,3} = -7 \pm j7$

are designed and presented in the Table I. The controllers are designed by defining the desired closed loop system characteristic (25) that includes the first order system part and the second order system part. Characteristic of the first order system is represented by the time constant (τ), while the second order system characteristic is represented by the system damping (ζ) and the natural frequency (ω_n).

The controller 1a is designed based on the following criteria: $\tau = 1$ second, $\zeta = 0.1$, and $\omega_n = 10$ rad/s. The controller 1a results in a closed loop system with eigenvalues: $\lambda_1 = -1$ and $\lambda_{2,3} = -2 \pm j9.798$. The λ_1 is located closer to the imaginary axis than the $\lambda_{2,3}$. It makes the closed loop system response to be dominated by the first order system part.

The controllers 1b and 1c are designed to have the same characteristic of the second order system part to the controller 1a, but different characteristic of the first order system part. The controller 1b is designed by defining $\tau = 0.2$ seconds, $\zeta = 0.1$, and $\omega_n = 10$ rad/s. The controller 1b results in a closed loop system with eigenvalues: $\lambda_1 = -5$ and $\lambda_{2,3} = -2 \pm j9.798$, where the $\lambda_{2,3}$ are located closer to the imaginary axis than the λ_1. The closed loop system response of using the controller 1b will be dominated by the second order system part. The controller 1c is designed based on the following criteria: $\tau = 0.1$ seconds, $\zeta = 0.1$, and $\omega_n = 10$ rad/s. Applying the controller 1c results in a closed loop system with eigenvalues: $\lambda_1 = -10$ and $\lambda_{2,3} = -2 \pm j9.798$. The controller 1c makes the closed loop system be more dominated by the second order system part than the controller 1b.

Simulation results of using the controllers 1a, 1b, and 1c on the TWR A for tracking the TWR B trajectory are shown in the Figures 2 and 3. Both figures shows that the three controllers were able to make the TWR A track the TWR B trajectory. The controller 1a required the longest time for TWR A to track the TWR B compared to the controllers 1b and 1c. The fastest tracking was achieved by the controller 1c but the TWR A trajectory showed an overshoot and oscillations. Tracking performance of the controller 1b was a little bit slower than the controller 1c but still much faster than the the controller 1a, but the controller 1b resulted in

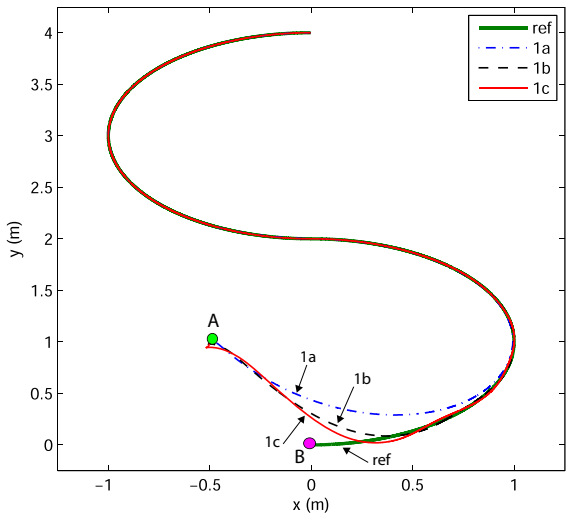

Fig. 2. Tracking control performance of using low-damping trajectory tracking control system.

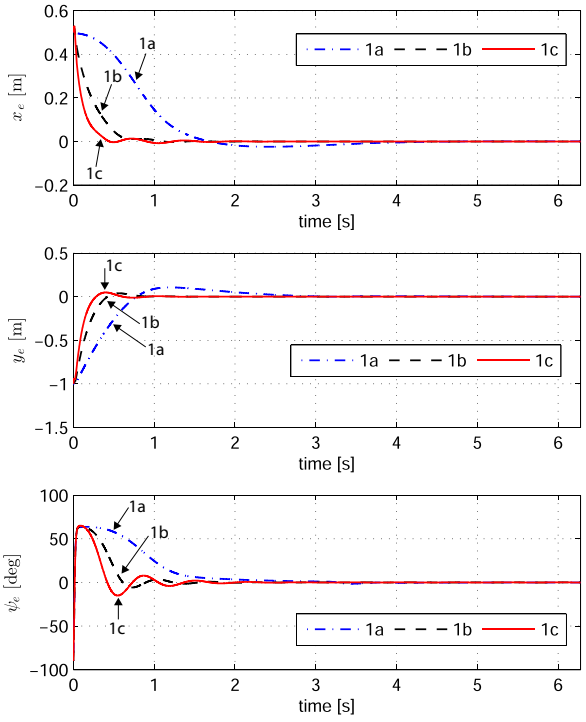

Fig. 3. Posture errors of using low-damping trajectory tracking control system.

very small overshoot. The Figure 3 shows the posture error of using the three controllers. The posture error of using controller 1a was decreasing very slow and required a long time period to converge zero. The controller 1a requires 4 seconds for the x_e, 2.8 seconds for the y_e, and 3.6 seconds for the ψ_e to converge zero. The posture error was converging to zero faster using the controller 1b than the controller 1a, i.e.: 1.3 seconds for x_e, 1 seconds for y_e, and 1.8 seconds for ψ_e. The controller 1b resulted in a small oscillation of the

ψ_e. The fastest decreasing posture error was achieved using the controller 1c, but it results in a significant oscillation on the ψ_e. The oscillation caused a longer time for the posture error convergence to zero. The converging time of the posture error using the controller 1c are 1.8 seconds for the x_e, 0.9 seconds for the y_e, and 1.8 seconds for the ψ_e. Comparing the trajectory tracking performance among the three controllers, the controller 1b shows the best tracking performance.

The controllers 1a, 1b, and 1c resulted in low-damping closed loop systems. Increasing the closed loop system damping is expected to result a better tracking performance. Therefore, three new controllers are designed and named the controllers 2a, 2b, and 2c as presented in the Table I. The three controllers are designed to have the same characteristic on second order system part but different characteristic on first order system part of the closed loop system. The second order system part of the closed loop systems is designed to have the system damping 0.7 and the frequency natural 10 rad/s. The first order system part of the closed loop systems is designed to have the time constant 1 second for the controller 2a, 0.2 seconds for the controller 2b, and 0.1 seconds for the controller 2c. Applying the three controllers result in the closed loop systems with same eigenvalues of the second order system part, $\lambda_{2,3} = -7 \pm j7$, but varying eigenvalue of the first order system part, i.e.: $\lambda_1 = -1$ for the controller 2a, $\lambda_1 = -5$ for the controller 2b, and $\lambda_1 = -10$ for the controller 2c.

Performances of the new controllers, 2a, 2b, and 2c, are demonstrated through computer simulations. The Figure 4 and Figure 5 show the simulation results of using the three controller and compared to the controller 1b performance. The Figure 4 shows the trajectories of TWR A and TWR B. The three new controllers were able to make the TWR A track the TWR B trajectory without overshoot. The controller 2c resulted in the fastest tracking followed by the controllers 2b and 2a, respectively. The Figure 5 shows time response of the posture errors during the simulations. The controller 2a resulted in 4 seconds for the x_e, 2.8 seconds for the y_e, and 2.8 seconds for the ψ_e to converge zero. The controller 2b resulted in the faster response than the controller 2a. Using the controller 2b, the x_e was converging to zero at 0.7 seconds, the y_e was converging zero at 0.6 seconds, and the ψ_e was converging zero at 1 second. The controller 2c resulted in the fastest time response among the three new controllers. Using the controller 2c, it needs 0.8 seconds for the x_e, 0.6 seconds for the y_e, and 0.9 seconds for the ψ_e to converge zero. Comparing the performance of the three new controllers, the controller 2c shows the best trajectory tracking performance.

Based on the simulation results, the controllers 1b and 2c resulted in the best tracking performance. Performance comparison of both controllers is given as follows. The Figure 4 shows that the TWR A trajectory was approaching the the TWR B trajectory almost at the same time by using the controllers 1b and 2c. The Figure 5 shows that the posture error of using the controller 2c was decreasing faster than using the controller 1b, but the posture error was converging to zero almost at the same time.

The simulation results using the six controllers show that domination of the second order system part of trajectory tracking control system results in better tracking performance

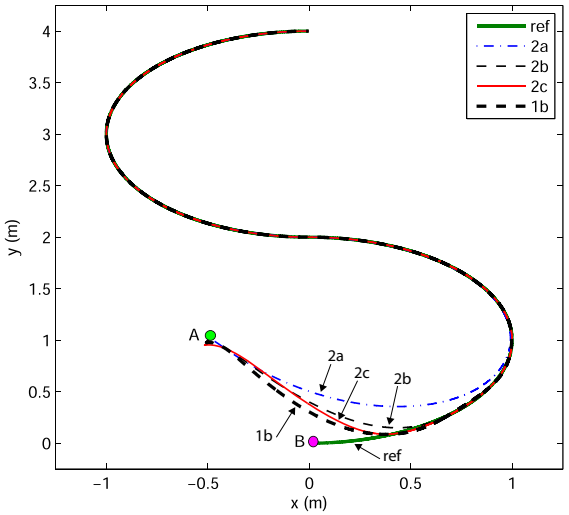

Fig. 4. Tracking control performance of using high-damping trajectory tracking control system.

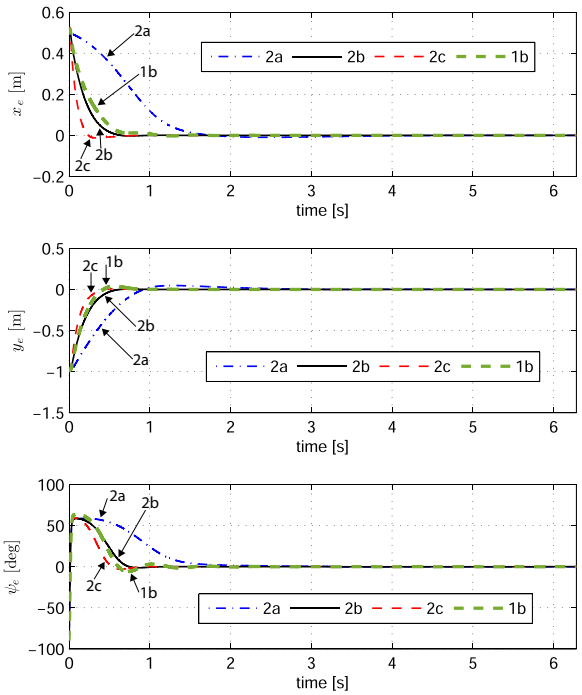

Fig. 5. Posture errors of using high-damping trajectory tracking control system.

than the domination of the first order system.

V. Discussion

It was presented a trajectory tracking control system (TTCS) design method based on poles domination approach in the previous section. The method is quite simple as a control gain of the TTCS is obtained directly through determining a desired closed loop system characteristic. The simulation results showed that the TTCS designed using the method were able to tracked the desired trajectories.

However, since the method was derived based on a linearized system, it results in locally asymptotic stable TTCS (LAS-TTCS). The LAS-TTCS works for a limited region of attraction such that the TTCS works in certain operating area of the robot.

A global asymptotically stable TTCS (GAS-TTCS) of mobile robot was presented in [1]. The GAS-TTCS has unbounded region of attraction such that it works for whole operating area of the robot. Control law of the GAS-TTCS was derived by applying the Lyapunov's stability theorem and rewritten as follows:

a. For the posture error dynamics (10), define the following positive definite function as a Lyapunov function candidate:

$$V = \frac{1}{2}\left(x_{e_A}^2 + y_{e_A}^2\right) + \frac{1}{c_0}\left(1 - \cos\psi_{e_A}\right) \tag{34}$$

where c_0 is a positive constant.

b. Differentiating the Lyapunov function candidate (34) with respect to time along trajectory of the posture error dynamics (10) results in:

$$\begin{aligned}
\dot{V} &= \dot{x}_{e_A}x_{e_A} + \dot{y}_{e_A}y_{e_A} + \frac{1}{c_0}\dot{\psi}_{e_A}\sin\psi_{e_A} \\
&= r_a x_{e_A} y_{e_A} + u_b x_{e_A}\cos\psi_{e_A} - u_a x_{e_A} \\
&\quad - r_a x_{e_A} y_{e_A} + u_b y_{e_A}\sin\psi_{e_A} \\
&\quad + \frac{1}{c_0}\left(r_b - r_a\right)\sin\psi_{e_A} \\
&= u_b x_{e_A}\cos\psi_{e_A} - u_a x_{e_A} + u_b y_{e_A}\sin\psi_{e_A} \\
&\quad + \frac{1}{c_0}\left(r_b - r_a\right)\sin\psi_{e_A} \\
&= \left(u_b\cos\psi_{e_A} - u_a\right)x_{e_A} \\
&\quad + \left[u_b y_{e_A} + \frac{1}{c_0}\left(r_b - r_a\right)\right]\sin\psi_{e_A}.
\end{aligned} \tag{35}$$

c. The posture error dynamics (10) is globally asymptotically stable (GAS) if the $\dot{V}$ in (35) is negative definite, $\dot{V} < 0$. The negative definiteness of $\dot{V}$ can achieved by the two following conditions:

$$u_a = u_b\cos\psi_{e_A} + c_1 x_{e_A} \tag{36}$$

and

$$r_a = r_b + c_0 u_b y_{e_A} + c_2\sin\psi_{e_A}, \tag{37}$$

where c_1 and c_2 are positive constants. The (36) and (37) are the states feedback control law of the GAS-TTCS. The control law has three unknown positive constants (c_0, c_1, and c_2) that are known as the GAS-TTCS control gains. The control gains are obtained through a trial and error process. The (37) is correcting the Kanayama's control law presented by the second part of equation (8) in [1].

Three controllers of the GAS-TTCS are designed as named by the controller 3a, the controller 3b, and the controller 3c, and listed in the Table II. Performances of the three GAS-TTCS controllers are evaluated through computer simulations. Performance of the three GAS-TTCS controllers are compared to the controller 2c and shown in the Figure 6 and Figure 7. The Figure 6 shows trajectory of the TWR A and the TWR B. It is shown that the controller 3c has the best tracking performance among the three GAS-TTCS controllers. The Figure 6 shows that the fastest tracking was

TABLE II
CONTROL GAIN OF GLOBAL ASYMPTOTICALLY STABLE TRAJECTORY TRACKING CONTROL SYSTEM (GAS-TTCS)

Controller	Control gain
3a	$c_0 = 10,\quad c_1 = 5,\quad c_2 = 5,$
3b	$c_0 = 30,\quad c_1 = 15,\quad c_2 = 10,$
3c	$c_0 = 50,\quad c_1 = 20,\quad c_2 = 10$

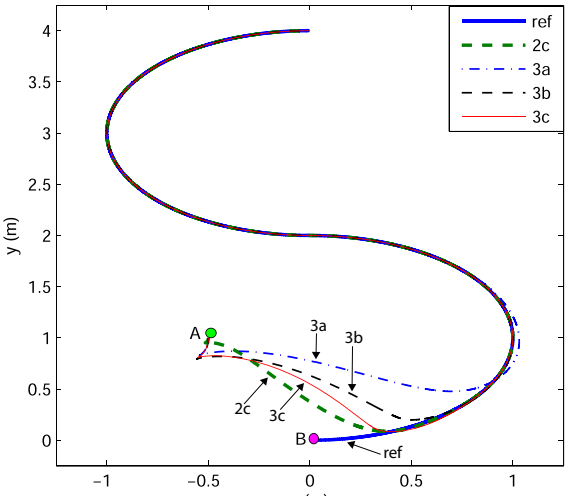

Fig. 6. Tracking control performance global asymptotically stable trajectory tracking control systems (3a, 3b, and 3c) versus high-damping locally asymptotically stable trajectory tracking control system (2c).

achieved by the controller 3c while the controller 3a resulted in the slowest tracking. It is confirmed by settling time of the posture error dynamics as shown in the Figure 7, in particularly for the y_e and ψ_e.

A further evaluation is done by comparing the performance of GAS-TTCS and LAS-TTCS. Performance of the controller 3c are compared to the performance of controller 2c. The controllers 3c and 2c are the designed controllers of the GAS-TTCS and LAS-TTCS, respectively, that have the best performance in this study. Performance comparison shows that both controllers has similar tracking performance as shown in the Figure 7 and the Figure 6. However, the controller 2c has better transient response than the controller 3c as shown in the Figure 7. The controller 2c resulted in less overshoot than the controller 3c for the x_e. Moreover, the controller 2c showed faster response than the controller 3c for the ψ_e. The GAS-TTCS assures the global tracking system but finding the proper control gain is not simple as it was done by trial and error. The LAS-TTCS achieves local tracking system only but the control gain is obtained in a simple and systematic using the pole domination approach. The simulation shows the LAS-TTCS has better performance than the GAS-TTCS. Applying the LAS-TTCS or GAS-TTCS depends on the application.

VI. CONCLUSION

A trajectory tracking control system (TTCS) of two-wheeled robot (TWR) has been designed using a control

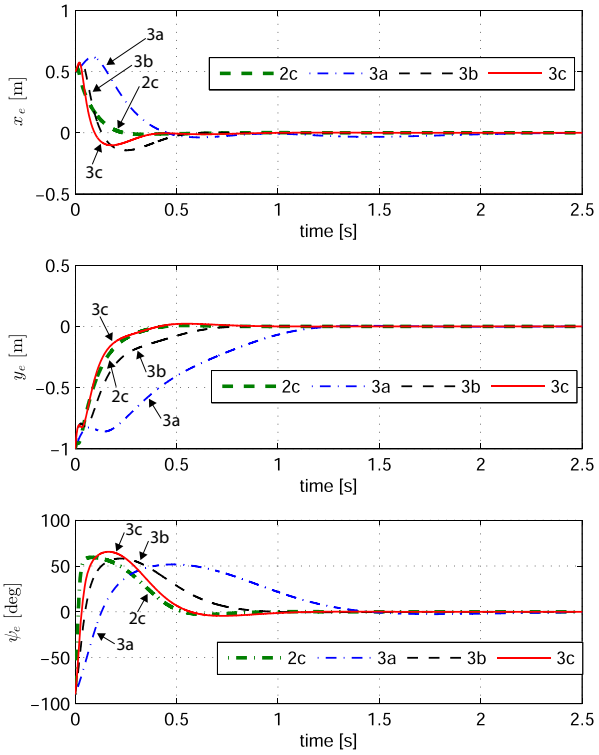

Fig. 7. Posture errors of using global asymptotically stable trajectory tracking control systems (3a, 3b, and 3c) versus high-damping locally asymptotically stable trajectory tracking control system (2c).

design method based pole domination approach. The method was derived by approximating the trajectory tracking control problem as a stabilization problem of third order linear system. A state feedback control was applied to stabilize the system. The state feedback control gain matrix was designed to have structure such that the closed loop system characteristic is fraction-able into a first order system part and the second order system part. The control gain matrix was designed by determining the desired characteristic of the first order and the second order system parts of the closed loop system. The method was applied in designing TTCS. Performance of the designed TTCS was evaluated through computer simulations. The simulation results show that the designed TTCS was able to track a desired trajectory. Moreover, domination of the second order system part in the closed loop system resulted in better performance than the domination of the first order system part. The control design method based pole domination approach provides a systematic method for designing a TTCS of TWR. The method resulted in a simple controller which is implementable in a low cost microcontroller.

VII. Future Works

The presented method is offering a simple way in designing a trajectory tracking control system of mobile robots. Since the method was derived based on the linearized system, region of attraction should be analyzed. Furthermore, this study will be continued to implement the designed trajectory tracking control system on a real two-wheeled robot system.

Acknowledgement

The author is very grateful to the Ministry of Research, Technology and Higher Education of the Republic of Indonesia for the financial support through the Program Bantuan Seminar Luar Negeri, Ditjen Penguatan Riset dan Pengembangan, Kemenristekdikti 2018 with number 3628/E5.3/PB/2018.

References

[1] Y. Kanayama, Y. Kimura, F. Miyazaki, and T. Noguchi, "A stable tracking control method for an autonomous mobile robot," in *Robotics and Automation, 1990. Proceedings., 1990 IEEE International Conference on*, pp. 384–389, IEEE, 1990.

[2] Z. P. Jiang and H. Nijmeijer, "Tracking control of mobile robots: A case study in backstepping," *Automatica*, vol. 33, no. 7, pp. 1393–1399, 1997.

[3] R. Dhaouadi and A. A. Hatab, "Dynamic modelling of differential-drive mobile robots using lagrange and newton-euler methodologies: A unified framework," *Advances in Robotics & Automation*, vol. 2, no. 2, pp. 1–7, 2013.

[4] Z.-P. Jiang, "Global tracking control of underactuated ships by lyapunov's direct method," *Automatica*, vol. 38, no. 2, pp. 301–309, 2002.

[5] F. Mazenc, K. Pettersen, and H. Nijmeijer, "Global uniform asymptotic stabilization of an underactuated surface vessel," *IEEE Transactions on Automatic Control*, vol. 47, no. 10, pp. 1759–1762, 2002.

[6] J. Xu, M. Wang, and L. Qiao, "Dynamical sliding mode control for the trajectory tracking of underactuated unmanned underwater vehicles," *Ocean engineering*, vol. 105, pp. 54–63, 2015.

[7] B. K. Sahu and B. Subudhi, "Adaptive tracking control of an autonomous underwater vehicle," *International Journal of Automation and Computing*, vol. 11, no. 3, pp. 299–307, 2014.

[8] B. Tutuko, S. Nurmaini, and P. S. Saparudin, "Route optimization of non-holonomic leader-follower control using dynamic particle swarm optimization," *IAENG International Journal of Computer Science*, vol. 46, no. 1, pp. 1–11, 2019.

[9] Y.-S. Ha *et al.*, "Trajectory tracking control for navigation of the inverse pendulum type self-contained mobile robot," *Robotics and autonomous systems*, vol. 17, no. 1-2, pp. 65–80, 1996.

[10] K. Pathak, J. Franch, and S. K. Agrawal, "Velocity and position control of a wheeled inverted pendulum by partial feedback linearization," *IEEE Transactions on robotics*, vol. 21, no. 3, pp. 505–513, 2005.

[11] R. Cui, J. Guo, and Z. Mao, "Adaptive backstepping control of wheeled inverted pendulums models," *Nonlinear Dynamics*, vol. 79, no. 1, pp. 501–511, 2015.

[12] M. Yue, S. Wang, and J.-Z. Sun, "Simultaneous balancing and trajectory tracking control for two-wheeled inverted pendulum vehicles: a composite control approach," *Neurocomputing*, vol. 191, pp. 44–54, 2016.

[13] C. Yang, Z. Li, R. Cui, and B. Xu, "Neural network-based motion control of an underactuated wheeled inverted pendulum model," *IEEE Transactions on Neural Networks and Learning Systems*, vol. 25, no. 11, pp. 2004–2016, 2014.

[14] M. Yue, C. An, and J.-Z. Sun, "An efficient model predictive control for trajectory tracking of wheeled inverted pendulum vehicles with various physical constraints," *International Journal of Control, Automation and Systems*, vol. 16, no. 1, pp. 265–274, 2018.

[15] N. Uddin, "Trajectory tracking control system design for autonomous two-wheeled robot," *Jurnal Infotel*, vol. 10, no. 3, pp. 90–97, 2018.

[16] T. Nomura, Y. Kitsuka, H. Suemitsu, and T. Matsuo, "Adaptive backstepping control for a two-wheeled autonomous robot," in *ICCAS-SICE, 2009*, pp. 4687–4692, IEEE, 2009.

[17] R. P. M. Chan, K. A. Stol, and C. R. Halkyard, "Review of modelling and control of two-wheeled robots," *Annual Reviews in Control*, vol. 37, no. 1, pp. 89–103, 2013.

[18] N. Uddin, "Lyapunov-based control system design of two-wheeled robot," in *Computer, Control, Informatics and its Applications (IC3INA), 2017 International Conference on*, pp. 121–125, IEEE, 2017.

[19] N. Uddin, T. A. Nugroho, and W. A. Pramudito, "Stabilizing two-wheeled robot using linear quadratic regulator and states estimation," in *Proc. of the 2nd International conferences on Information Technology, Information Systems and Electrical Engineering (ICITISEE)*, (Yogyakarta, Indonesia), Oct. 2017.

[20] N. Uddin, "A robot trajectory tracking control system design using pole domination approach," in *2018 IEEE 9th Annual Information Technology, Electronics and Mobile Communication Conference (IEMCON)*, (Vancouver), pp. 506–512, Nov 2018.